Int J Clin Exp Pathol 2014;7(11):7545-7553
www.ijcep.com /ISSN:1936-2625/IJCEP0002571

Original Article

Isolation of myeloid-derived suppressor cells subsets from spleens of orthotopic liver cancer-bearing mice by fluorescent-activated and magnetic-activated cell sorting: similarities and differences

Yaping Xu*, Wenxiu Zhao*, Duan Wu, Jianfeng Xu, Suqiong Lin, Kai Tang, Zhenyu Yin, Xiaomin Wang

*Department of Hepatobiliary Surgery, Zhongshan Hospital, Xiamen University, Fujian Provincial Key Laboratory of Chronic Liver Disease and Hepatocellular Carcinoma (Xiamen University Affiliated Zhongshan Hospital), Xiamen, China. *Equal contributors.*

Received September 17, 2014; Accepted November 1, 2014; Epub October 15, 2014; Published November 1, 2014

Abstract: Myeloid-derived suppressor cells (MDSCs) are a heterogeneous population of immature myeloid cells that commonly expand during tumor development and that play a critical role in suppression of immune responses. MDSCs can be classified into two groups: Mo-MDSCs and G-MDSCs. These cells differ in their morphology, phenotype, differentiation ability, and immunosuppressive activity, and inhibit immune responses via different mechanisms. Therefore, identifying an effective method for isolating viable Mo-MDSCs and G-MDSCs is important. Here, we demonstrated the differences and similarities between fluorescence-activated cell sorting (FACS) and magnetic-activated cell sorting (MACS) in sorting G-MDSCs and Mo-MDSCs. Both MACS and FACS could obtain G-MDSCs and Mo-MDSCs with high viability and purity. A high yield and purity of G-MDSCs could be obtained both by using FACS and MACS, because G-MDSCs are highly expressed in the spleen of tumor-bearing mice. However, Mo-MDSCs, which comprise a small population among leukocytes, when sorted by MACS, could be obtained at much greater cell number, although with a slightly lower purity, than when sorted by FACS. In conclusion, we recommended using both FACS and MACS for isolating G-MDSCs, and using MACS for isolation of Mo-MDSCs.

Keywords: Fluorescent-activated cell sorting (FACS), granulocytic, magnetic-activated cell sorting (MACS), monocytic, myeloid-derived suppressor cell, separation

Introduction

Myeloid-derived suppressor cells (MDSCs), a newly identified kind of immune inhibitory cell, play an important role in the tumor immune-escape process [1]. MDSCs are one of the main populations of myeloid cells, comprising progenitor cells, immature macrophages, immature granulocytes, and immature dendritic cells [2]. In mice, these cells are commonly defined as $CD11b^{+}Gr\text{-}1^{+}$ cells [3-5], which consist of two major subsets: $Ly6G^{+}Ly6C^{low}$ granulocytic MDSCs (G-MDSCs) and $Ly6G^{-}Ly6C^{high}$ monocytic MDSCs (Mo-MDSCs) [4, 6]. In most tumor models, the expansion of MDSCs predominantly involves G-MDSCs (70-80%) [4, 7]. Importantly, these two subsets of cells inactivate the immune response via different mechanisms [8, 9]. G-MDSCs produce increased levels of reactive oxygen species (ROS) and undetectable levels of nitric oxide (NO), whereas Mo-MDSCs generate increased levels of NO, but undetectable levels of ROS [4, 10-13].

It has been reported that, in some tumor models systems, the relative frequency of Mo-MDSCs, as compared to G-MDSCs, is reduced in the blood compared to the spleen (1:11 blood versus 1:5 spleen), and that this relative frequency is the lowest in the tumor (1:113) [14]. The percentages of Mo-MDSC are significantly less in immune organs in comparison with those of G-MDSCs in tumor-bearing mice. This poses a challenge for obtaining sufficient cells for analyses. Therefore, an efficient method for separating G-MDSCs and Mo-MDSCs is in great demand.

At present, there are some feasible ways for obtaining subsets of MDSCs. 1) A phycoerythrin (PE)-positive Isolation Kit (STEMCELL Technologies; Vancouver, Canada) [15]; 2) Myeloid-Derived Suppressor Cell Isolation Kit for mouse MDSCs via magnetic-activated cell sorting (MACS) from Miltenyi Biotec (Bergisch Gladbach, Germany) [16]; 3) fluorescence-activated cell sorting (FACS) [17]. However, the relative efficiency of these methods has not been investigated to date.

In the present study, we compared FACS and MACS methods for obtaining pure $CD11b^{+}Ly6G^{+}Ly6C^{low}$ G-MDSCs and $CD11b^{+}Ly6G^{-}Ly6C^{high}$ Mo-MDSCs, and analyzed the cell survival rate, cell purity, and cell yield.

Materials and methods

Animals and cell lines

All experimental protocols were reviewed and approved by our institutional review board. All animal experimental protocols were performed in compliance with the Guidelines for the Institutional Animal Care and Use Committee of Xiamen University.

BALB/c (H-2d, haplotype) mice were purchased from the National Rodent Laboratory Animal Resources, Shanghai, China. Adult male animals, aged 8-12 weeks, were used. The mouse hepatoma cell line, H22, was purchased from Shanghai Cell Bank, Chinese Academy of Sciences, and was maintained in RPMI 1640 (HyClone, Beijing, China), supplemented with 10% fetal bovine serum (FBS), 100 U/mL penicillin, and 100 μg/mL streptomycin, as previously described [18].

In situ hepatic tumor model

The HCC model was created by direct intrahepatic injection of mouse hepatoma H22 cells (originating from BALB/c mice of the H-2d haplotype), as previously described [19]. Mice were anesthetized by intraperitoneal injection of 5% chloral hydrate (0.1 mL/10 g body weight), and opened via a midline incision to expose the liver. One million H22 cells, suspended in 30-50 μL of phosphate-buffered saline (PBS) was slowly injected under the hepatic capsule into the upper left lobe of the liver, using a 28-gauge needle. A pale, whitish coloring could be observed at the point of injection under the hepatic capsule. A gentle compression was applied for 30 s with a cotton applicator to avoid bleeding and reflux of the cells. The abdomen was closed with a 5-0 silk suture. The mice were observed for 2-3 h and then returned to the storage facilities. Ten days later the mice were sacrificed and the anatomy studied.

Separation of spleen cells

Splenocytes were isolated from the spleens of tumor-bearing mice by disaggregation into 10 mL of RPMI 1640 complete medium. Erythrocytes were lysed with Red Blood Cell Lysis Buffer (Beyotime, Nanjing, China). Then, splenocytes were mashed through 70-μm cell strainers to obtain single-cell suspensions.

MACS separation

For MACS separation, the MDSC Isolation Kit (Miltenyi Biotec, Bergisch Gladbach, Germany) and biotinylated rat anti-mouse Ly6G and Ly6C (BD Biosciences, San Jose, CA) were used.

G-MDSCs were isolated according to the manufacturer's instructions (MDSC kit). For Ly6G separation, up to 1×10^8 total cells were centrifuged at 300 × *g* for 10 min at 4°C. The cell pellets were resuspended in 700 μL of PBS (pH 7.2), 0.5% bovine serum albumin (BSA), and 2 mM EDTA. FCR blocking reagent (50 μL) was added, mixed well, and incubated for 10 min at 4°C. After incubation, 100 μL of biotin-conjugated anti-Ly6G antibody was added and the cells incubated for a further 15 min at 4°C. Cells were washed by adding 10 mL of buffer and centrifuging at 300 × *g* for 10 min at 4°C. The labeled cells were resuspended in 800 μL of buffer; then, 200 μL of anti-biotin microbeads was added, mixed well, and incubated for 10 min at 4°C. Cells were washed by adding 10-20 mL of buffer and centrifuging at 300 × *g* for 10 min at 4°C. The cell pellets were then resuspended in 500 μL of buffer.

For separation of Mo-MDSCs, the cells remaining after the Ly6G-separation were centrifuged at 300 × *g* for 10 min at 4°C. The cell pellet was resuspended in 400 μL of buffer, after which 10 μL of biotin-conjugated rat anti-mouse Ly6G and Ly6C antibodies was added (BD Biosciences, San Jose, CA). Samples were mixed well and incubated for 10 min at 4°C. Cells were then washed by adding 10 μL of buffer and centrifuging at 300 × *g* for 10 min at 4°C.

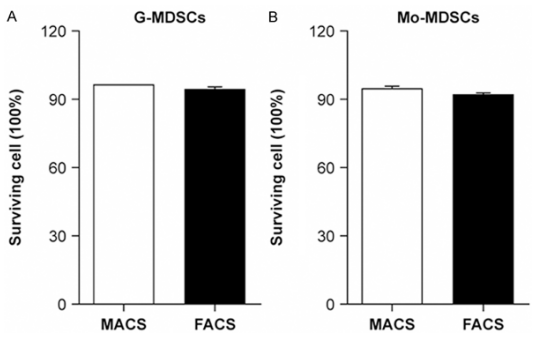

Figure 1. Cell survival rates after magnetic-activated cell sorting (MACS) and fluorescent-activated cell sorting (FACS) separation. For MACS separation (blank column), about 5%, and for FACS separation (black column), about 8%, of the initially applied G-MDSCs cells had died. For Mo-MDSCs, the viability was about 92% for MACS-separated, and about 90% for FACS-separated cells. The difference between the survival/mortality rates obtained by the two separation methods (n = 3 for each separation method) was not statistically significant ($P = 0.2$).

The cell pellet was resuspended in 900 μL of buffer, to which was added 100 μL of streptavidin micobeads. Samples were mixed well and incubated for 15 min at 4°C. Cells were washed again by adding 10-20 mL of buffer and centrifuging at 300 × *g* for 10 min at 4°C. The cell pellet was resuspended in 500 μL of buffer, and magnetic separation (2.5) was then performed as the instructions supplied by the MDSC kit. The collected cells were Gr-1^{low}Ly6C^{high}.

FACS separation

For flow cytometric sorting, 1 × 10^7 cells/mL splenocytes from tumor-bearing mice were stained with anti-CD11b-APC (BD Biosciences), anti-Ly6G-FITC (BD Biosciences), and anti-Ly6C-PE (BD Biosciences) antibodies for 20 min on ice in staining buffer (1% FBS in PBS). Cells were then washed with PBS, and the samples were then sorted using a BD Influx. To obtain pure cells, the *1.5 drop pure* sort mode was chosen. The cells were sorted by gating on P1 (CD11b$^+$Ly6G$^-$Ly6C^{high}) as well as by gating on P2 (CD11b$^+$Ly6G$^+$Ly6C^{low}).

Analysis of purity of cells separated by MACS and FACS

After the magnetic separation, cells were labeled with APC-conjugated anti-CD11b, FITC-conjugated anti-Ly6G, and PE-conjugated anti-Ly6C antibodies, and were analyzed by FACS. Cells separated by flow cytometry were analyzed immediately. The purity of G-MDSCs was calculated using the formula CD11b$^+$% × CD11b$^+$Ly6G$^+$Ly6C^{low}%, while that of Mo-MDSCs was CD11b$^+$% × CD11b$^+$Ly6G$^-$Ly6C$^+$%.

Analysis of the survival of MACS- and FACS-separated cells

Immediately after sorting, cells were detected, and the number and the survival rate determined using an ADAM-MC (Digital Bio Technology, Seoul, Korea) according to the manufacturer's instructions.

Wright-Giemsa stain for determining MDSC morphology

Cell smears were prepared on sterile slides and air dried, where after the cells were stained with Wright-Giemsa stain solution for 3-4 min, followed by addition of 2.0 mL of distilled water for 5-10 min; the latter step was repeated once more. The slides were rinsed with water until the edges were a pinkish red, and were then air-dried.

Statistical analysis

Experiments were performed at least three times. Results are expressed as means ± SD. The data were analyzed using SPSS software (v. 13.0). Statistical analyses were performed using Student's *t*-test. The significance level was set at 0.05.

Results

Determination of cell viability after MDSCs and FACS

The population of G-MDSCs and Mo-MDSCs among splenocytes obtained from tumor-bearing mice was determined before separation. After separation, the viability of the cells was calculated using an Automated Cell Counter. As shown in **Figure 1A**, the viability of G-MDSCs was 96.33 ± 3.33% by MACS separation and 93.33 ± 1.70% by FACS separation. The viability of Mo-MDSCs was slightly decreased compared with that of G-MDSCs, viz., 94.00 ± 1.00% and 90.67 ± 1.20% by FACS and MACS, respectively (**Figure 1B**). There was no statistically significant difference in cell viability between the two separation methods.

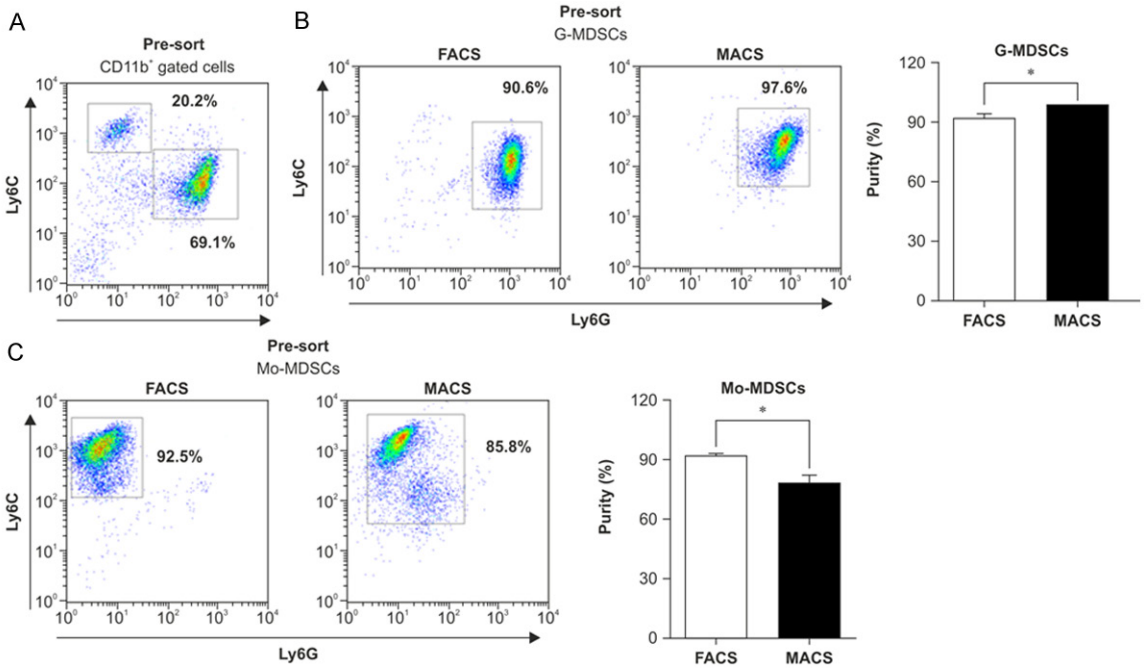

Figure 2. Purity of fluorescent-activated cell sorting (FACS) - and magnetic-activated cell sorting (MACS)-separated G-MDSCs and Mo-MDSCs were determined by flow cytometric analysis. After separation, the cells were labeled with fluorescently labeled anti-CD11b, anti-Ly6G, and anti-Ly6C antibodies, and the purity of the cells analyzed by flow cytometry. (A) Before sorting, the ratio of G-MDSCs to Mo-MDSCs was about 1:3 among the $CD11b^+$ cells obtained from the spleens of tumor-bearing mice. (B, C) Representative flow cytometry dot plots and quantitative data showing the purity of G-MDSCs (B) and Mo-MDSCs (C).

Analysis of cell purity of MACS- and FACS-separated cell fractions

Next, we assessed the purity of the separated G-MDSCs and Mo-MDSCs by flow cytometry. Cells separated by MACS were labeled with APC-conjugated anti-CD11b, FITC-conjugated anti-Ly6G, and PE-conjugated anti-Ly6C antibodies. After FACS, the sorted cells were analyzed immediately by flow cytometry. As shown in **Figure 2A**, the percentage of G-MDSCs and Mo-MDSCs of splenocytes was 69.00% and 23.00%, and the ratio of G-MDSCs to Mo-MDSCs was 3:1. Previously, this ratio has been reported to be about 5:1 [4]. The difference in these ratios may be due to the different tumor models used in our and previous reports.

After FACS and MACS separation, the percentage of G-MDSCs ($CD11b^+Ly6G^+Ly6C^{low}$) in the context of the total cell number was 89.87 ± 0.94% and 97.60 ± 1.03%, respectively. The purity of G-MDSCs exceeded 90% after both MACS and FACS separation; the purity obtained by MACS separation was moderately higher than that achieved by FACS ($P < 0.05$). However, when comparing the purity of Mo-MDSCs obtained by means of MACS and FACS, the purity of Mo-MDSCs separated by MACS was significantly lower than that of these cells sorted by FACS ($P < 0.05$; 85.80% by MACS vs. 92.50% by FACS).

Morphological analysis of G-MDSCs and Mo-MDSCs sorted by FACS and MACS

We next analyzed the morphology of G-MDSCs and Mo-MDSCs sorted by FACS and MACS. As shown in **Figure 3**, the cell morphology of G-MDSCs and Mo-MDSCs isolated by these two methods was similar. The G-MDSCs were generally smaller in size, with a higher nucleus-to-cytoplasm ratio, a transparent blue cytoplasm, and were multinuclear or band granulocytes (**Figure 3A**). On the other hand, the Mo-MDSCs separated by FACS and MACS were large and immature in appearance, and had bean-shaped nuclei that were unilobar, with some vacuoles present in the cytoplasm.

Redetection of Mo-MDSCs separated by FACS and MACS

After sorting, the cells were stained with APC-conjugated anti-CD11b, FITC-conjugated anti-

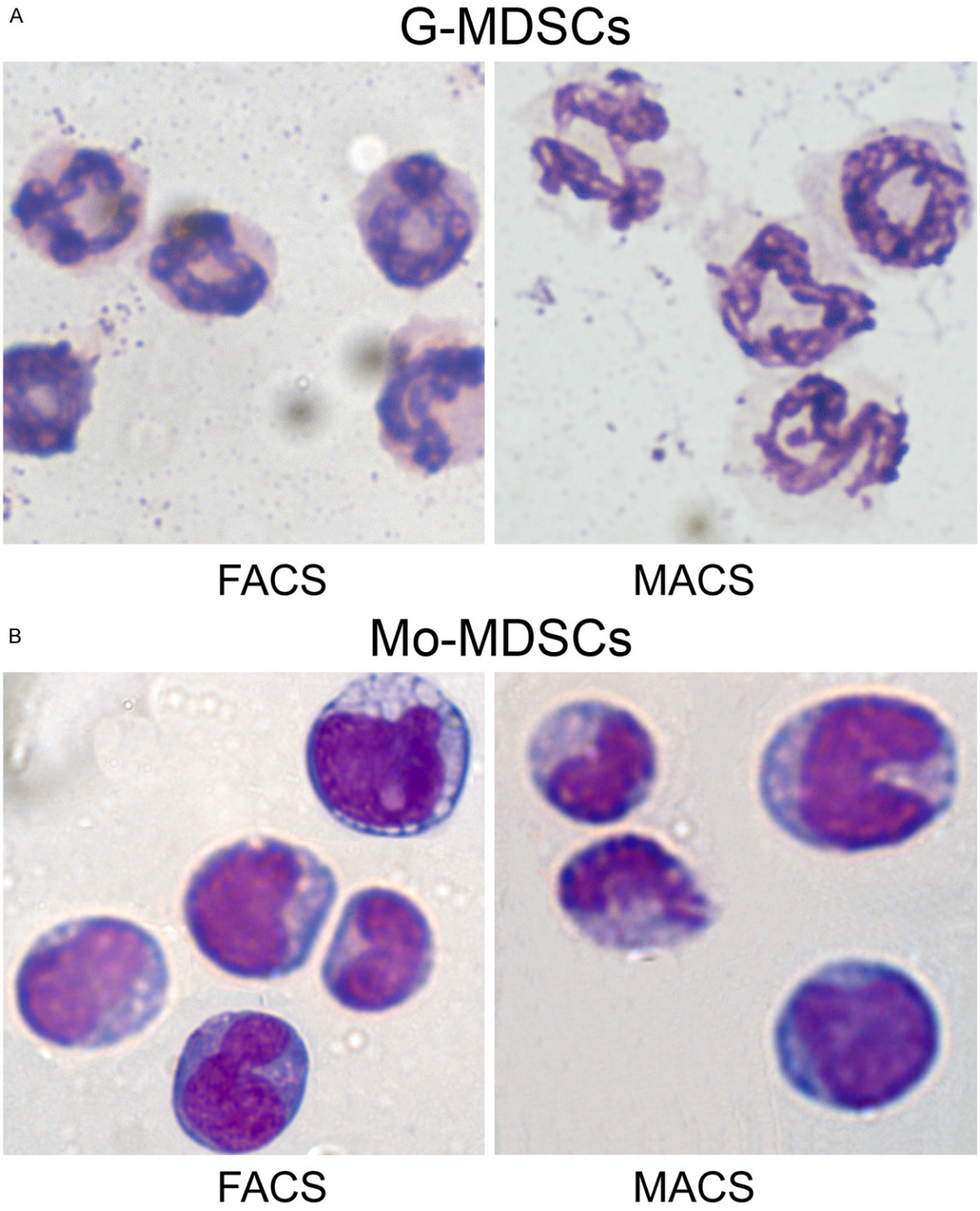

Figure 3. Wright-Giemsa staining of cells purified by fluorescent-activated cell sorting (FACS) and magnetic-activated cell sorting (MACS). A. G-MDSCs purified by FACS and MACS stained with Wright-Giemsa stain showed the same appearance and were generally smaller in size, with a higher nucleus-to-cytoplasm ratio. B. Mo-MDSCs showed features of immature monocytes. Magnification, 1,000 ×. Similar data were obtained in three additional experiments.

Ly6G, and PE-conjugated anti-Ly6C antibodies, and were then detected by flow cytometry. Mo-MDSCs separated by MACS comprised two subsets ($CD11b^{+}Ly6G^{-}Ly6C^{high}$ and $CD11b^{+}Ly6G^{-}Ly6C^{low}$), compared to those separated by FACS, which comprised only $CD11b^{+}Ly6G^{-}Ly6C^{high}$ cells (**Figure 4**). We gated the cells of interest and then sorted them using FACS. As

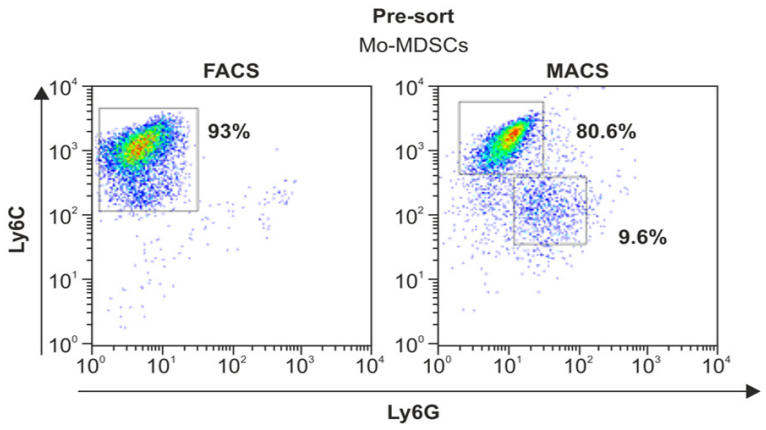

Figure 4. Mo-MDSCs separated by fluorescent-activated cell sorting (FACS) and magnetic-activated cell sorting (MACS). Mo-MDSCs separated by MACS comprised two subsets ($CD11b^+$ $Ly6G^-Ly6C^{high}$ and $CD11b^+$ $Ly6G^-Ly6C^{low}$), while those separated by FACS comprised only $CD11b^+$ $Ly6G^-Ly6C^{high}$ cells.

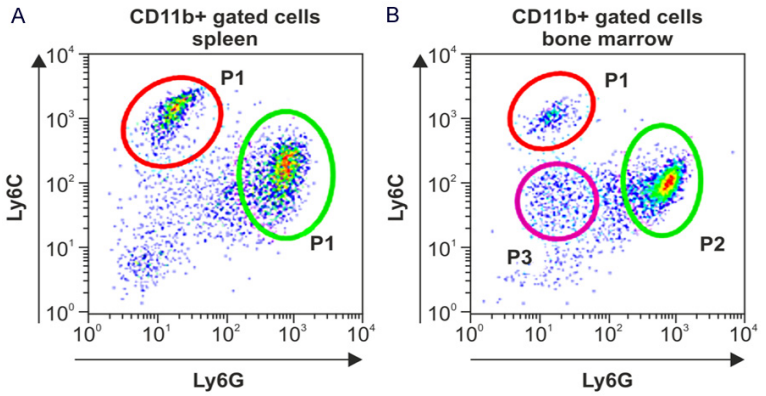

Figure 5. MDSC subset populations in spleen and bone marrow of tumor-bearing mice. A. When separating Mo-MDSCs and G-MDSCs by fluorescent-activated cell sorting (FACS), we selected P1 to sort Mo-MDSCs, and P2 to sort G-MDSCs. B. The G-MDSCs and Mo-MDSCs in the bone marrow of tumor-bearing mice comprised three subsets of populations. P1 gated the $CD11b^+Ly6G^-Ly6C^{high}$, P2 gated the $CD11b^+Ly6G^+Ly6C^{low}$ and P3 gated the $CD11b^+Ly6G^-Ly6C^{low}$ cells.

shown in **Figure 5**, markedly more cells obtained from bone marrow expressed $CD11b^+Ly6G^-Ly6C^{low}$ than did cells obtained from spleen.

Discussion

During the past decade, numerous studies have shown that MDSCs accumulate during tumor progression, traumatic stress, chronic infections, and psychological stress [20-22]. It is now well established that MDSCs can be classified into two groups of cells, viz., Mo-MDSCs and G-MDSCs. In mice, Mo-MDSCs are $CD11b^+Ly6G^-Ly6C^{high}$, while G-MDSCs are $CD11b^+Ly6G^+Ly6C^{low}$ [23, 24]. In addition to differences in morphology and phenotype, these groups differ in gene expression profiles, immunosuppressive activity, and the mechanism by which they inhibit immune responses [4, 25, 26]. In this study, we attempted to clarify the differences and similarities between FACS and MACS approaches to sorting G-MDSCs and Mo-MDSCs, in order to find effective methods that can facilitate further research into these cells.

To address this question, we compared FACS and MACS methods to separate G-MDSCs and Mo-MDSCs from the spleens of orthotopic (H22) liver cancer-bearing mice. We characterized murine G-MDSCs and Mo-MDSCs using APC-conjugated CD11b, FITC-conjugated Ly6G, and PE-conjugated Ly6C antibodies by flow cytometry. For MACS isolation, a commercial but modified MDSC isolation kit from Miltenyi Biotec was used. As shown in **Figure 1**, the viability of G-MDSCs and Mo-MDSCs obtained by FACS and MACS both exceeded 90%, which demonstrated that both FACS and MACS were gentle on the cells, although of course adequate preparation and appropriate buffers were necessary for cell suspension and separation. In addition, when staining cells with antibodies, 1% BSA and 2 mM EDTA in 1 × PBS was strongly recommended as a staining buffer to prevent non-specific binding, cell adherence, and retain the viability of the cells. Moreover, the low concentration of animal serum proteins in this solution maintains the viability of the cells [27].

To determine which method was more appropriate for separating G-MDSCs and Mo-MDSCs, we compared the purity of G-MDSCs and Mo-MDSCs that had been separated by FACS and MACS. Given that the purity of G-MDSCs exceeded 90% for both MACS and FACS sepa-

ration, it appears that both FACS and MACS are suitable for sorting G-MDSCs (**Figure 2B**). The purity of Mo-MDSCs sorted by MACS was slightly lower than those of cells sorted by FACS (85.5% vs. 92.5%; $P < 0.05$; **Figure 2C**). However, sorting cells by MACS can save time. For example, to obtain about 1×10^6 Mo-MDSCs requires approximately 4 h by MACS, whereas it would take 10 h by FACS. Sorting by MACS is also more costly.

Interestingly, when using magnetic beads, we obtained two subsets of Mo-MDSCs, viz., $CD11b^+Ly6G^-Ly6C^{high}$ and $CD11b^+Ly6G^-Ly6C^{low}$, but only obtained a single subset of Mo-MDSCs $CD11b^+Ly6G^-Ly6C^{high}$, when using flow sorting (**Figure 4**). In FACS, we gated the cells of interest prior to sorting. As shown in **Figure 5**, cells obtained from bone marrow more often expressed $CD11b^+Ly6G^-Ly6C^{low}$ than did cells obtained from spleen. When sorting Mo-MDSCs from among splenocytes, only P1 ($CD11b^+Ly6G^-Ly6C^{high}$) cells were sorted and P3 cells ($CD11b^+Ly6G^-Ly6C^{low}$) were ignored.

The RB6-8C5, an anti-Gr-1 monoclonal antibody, reacts with a common epitope on Ly-6G and Ly-6C, is widely used for depletion of $Gr\text{-}1^+$ MDSCs, including hepatic MDSCs, by many investigators [28-32]. When sorting Mo-MDSCs using the commercial MDSC isolation kit from Miltenyi Biotec, Mo-MDSC was incubated with the biotinylated anti-Gr-1 antibody involved in the kit and the yield of Mo-MDSCs was very low. Using a biotinylated anti-Gr-1 (RB6-8C5) antibody from BD Biosciences markedly up-regulated the yield of Mo-MDSCs, demonstrating that anti-Gr-1 antibody from BD Biosciences showed stronger binding to Ly6C than did the antibody from Miltenyi Biotec. Thus, the biotinylated anti-Gr-1 (RB6-8C5) antibody from BD Biosciences is strongly recommended for use in sorting Mo-MDSCs. Moreover, after incubation with biotinylated anti-Gr-1 antibody, streptavidin magnetic beads were applied according to the kit, as the streptavidin molecule is said to possess more binding sites than the biotinylated molecule, thus resulting in stronger and better magnetic labeling. Compared with Mo-MDSCs separated by FACS and the PE-positive isolation kit, Mo-MDSCs separated using the modified MDSC kit is advantageous, as it allows for additional staining and high-speed sorting.

In summary, G-MDSCs and Mo-MDSCs sorted by either FACS or MACS with high viability and purity can be used in functional and non-functional studies. Due to the high percentage of G-MDSCs in the spleens of tumor-bearing mice, both FACS and MACS could be used to obtain a high yield and purity of G-MDSCs, but using FACS could do so in less time and at lower cost than using MACS. For sorting low abundance cell populations, such as Mo-MDSCs, MACS is recommended, although the purity of the Mo-MDSCs sorted by MACS was slightly lower than that obtained by FACS, the number of cells isolated in the equivalent amount of time was much higher. In conclusion, we recommended using both FACS and MACS for isolation of G-MDSCs, and using MACS for isolation of Mo-MDSCs.

Acknowledgements

We thank Ms. Qin Yao and Ms. Huiqin Zhuo for their help with flow cytometry. This study was supported by grants from the National Key Sci-Tech Special Project of China (No. 2012-Zx10002-011-005), the National Natural Science Foundation of China (No. 81171976 and No. 81201894), and Projects of Xiamen Science and Technology Program (3502Z2013-0030).

Disclosure of conflict of interest

None.

Address correspondence to: Dr. Xiaomin Wang or Zhenyu Yin, Department of Hepatobiliary Surgery, Zhongshan Hospital, Xiamen University, Fujian Provincial Key Laboratory of Chronic Liver Disease and Hepatocellular Carcinoma (Xiamen University Affiliated Zhongshan Hospital), South Hubin Road #209, Xiamen 361004, China. E-mail: wxm2203@xmu.edu.cn (XMW); yinzy@xmu.edu.cn (ZYY)

References

[1] Sevko A and Umansky V. Myeloid-derived suppressor cells interact with tumors in terms of myelopoiesis, tumorigenesis and immunosuppression: thick as thieves. J Cancer 2013; 4: 3-11.

[2] Kusmartsev S and Gabrilovich DI. Role of immature myeloid cells in mechanisms of immune evasion in cancer. Cancer Immunol Immunother 2006; 55: 237-245.

[3] Gabrilovich DI, Bronte V, Chen SH, Colombo MP, Ochoa A, Ostrand-Rosenberg S and Schreiber H. The terminology issue for myeloid-

derived suppressor cells. Cancer Res 2007; 67: 425; author reply 426.
[4] Youn JI, Nagaraj S, Collazo M and Gabrilovich DI. Subsets of myeloid-derived suppressor cells in tumor-bearing mice. J Immunol 2008; 181: 5791-5802.
[5] Gabrilovich DI and Nagaraj S. Myeloid-derived suppressor cells as regulators of the immune system. Nat Rev Immunol 2009; 9: 162-174.
[6] Hestdal K, Ruscetti FW, Ihle JN, Jacobsen SE, Dubois CM, Kopp WC, Longo DL and Keller JR. Characterization and regulation of RB6-8C5 antigen expression on murine bone marrow cells. J Immunol 1991; 147: 22-28.
[7] Zea AH, Rodriguez PC, Atkins MB, Hernandez C, Signoretti S, Zabaleta J, McDermott D, Quiceno D, Youmans A, O'Neill A, Mier J and Ochoa AC. Arginase-producing myeloid suppressor cells in renal cell carcinoma patients: a mechanism of tumor evasion. Cancer Res 2005; 65: 3044-3048.
[8] Talmadge JE. Pathways mediating the expansion and immunosuppressive activity of myeloid-derived suppressor cells and their relevance to cancer therapy. Clin Cancer Res 2007; 13: 5243-5248.
[9] Sui Y, Hogg A, Wang Y, Frey B, Yu H, Xia Z, Venzon D, McKinnon K, Smedley J, Gathuka M, Klinman D, Keele BF, Langermann S, Liu L, Franchini G and Berzofsky JA. Vaccine-induced myeloid cell population dampens protective immunity to SIV. J Clin Invest 2014; 124: 2538-2549.
[10] Luyckx A, Schouppe E, Rutgeerts O, Lenaerts C, Koks C, Fevery S, Devos T, Dierickx D, Waer M, Van Ginderachter JA and Billiau AD. Subset characterization of myeloid-derived suppressor cells arising during induction of BM chimerism in mice. Bone Marrow Transplant 2012; 47: 985-992.
[11] Kostlin N, Kugel H, Spring B, Leiber A, Marme A, Henes M, Rieber N, Hartl D, Poets CF and Gille C. Granulocytic myeloid derived suppressor cells expand in human pregnancy and modulate T-cell responses. Eur J Immunol 2014; 44: 2582-2591.
[12] Trikha P and Carson WE 3rd. Signaling pathways involved in MDSC regulation. Biochim Biophys Acta 2014; 1846: 55-65.
[13] Filipazzi P, Valenti R, Huber V, Pilla L, Canese P, Iero M, Castelli C, Mariani L, Parmiani G and Rivoltini L. Identification of a new subset of myeloid suppressor cells in peripheral blood of melanoma patients with modulation by a granulocyte-macrophage colony-stimulation factor-based antitumor vaccine. J Clin Oncol 2007; 25: 2546-2553.
[14] Highfill SL, Cui Y, Giles AJ, Smith JP, Zhang H, Morse E, Kaplan RN and Mackall CL. Disruption of CXCR2-mediated MDSC tumor trafficking enhances anti-PD1 efficacy. Sci Transl Med 2014; 6: 237ra267.
[15] Raber PL, Thevenot P, Sierra R, Wyczechowska D, Halle D, Ramirez ME, Ochoa AC, Fletcher M, Velasco C, Wilk A, Reiss K and Rodriguez PC. Subpopulations of myeloid-derived suppressor cells impair T cell responses through independent nitric oxide-related pathways. Int J Cancer 2014; 134: 2853-2864.
[16] Su H, Cong X and Liu YL. Transplantation of granulocytic myeloid-derived suppressor cells (G-MDSCs) could reduce colitis in experimental murine models. J Dig Dis 2013; 14: 251-258.
[17] Schlecker E, Stojanovic A, Eisen C, Quack C, Falk CS, Umansky V and Cerwenka A. Tumor-infiltrating monocytic myeloid-derived suppressor cells mediate CCR5-dependent recruitment of regulatory T cells favoring tumor growth. J Immunol 2012; 189: 5602-5611.
[18] Zhao W, Zhang L, Xu Y, Zhang Z, Ren G, Tang K, Kuang P, Zhao B, Yin Z and Wang X. Hepatic stellate cells promote tumor progression by enhancement of immunosuppressive cells in an orthotopic liver tumor mouse model. Lab Invest 2014; 94: 182-191.
[19] Kuang P, Zhao W, Su W, Zhang Z, Zhang L, Liu J, Ren G, Yin Z and Wang X. 18beta-glycyrrhetinic acid inhibits hepatocellular carcinoma development by reversing hepatic stellate cell-mediated immunosuppression in mice. Int J Cancer 2013; 132: 1831-1841.
[20] Serafini P, Borrello I and Bronte V. Myeloid suppressor cells in cancer: recruitment, phenotype, properties, and mechanisms of immune suppression. Semin Cancer Biol 2006; 16: 53-65.
[21] Makarenkova VP, Bansal V, Matta BM, Perez LA and Ochoa JB. CD11b+/Gr-1+ myeloid suppressor cells cause T cell dysfunction after traumatic stress. J Immunol 2006; 176: 2085-2094.
[22] Jin J, Wang X, Wang Q, Guo X, Cao J, Zhang X, Zhu T, Zhang D, Wang W, Wang J, Shen B, Gao X, Shi Y and Zhang J. Chronic psychological stress induces the accumulation of myeloid-derived suppressor cells in mice. PLoS One 2013; 8: e74497.
[23] Peranzoni E, Zilio S, Marigo I, Dolcetti L, Zanovello P, Mandruzzato S and Bronte V. Myeloid-derived suppressor cell heterogeneity and subset definition. Curr Opin Immunol 2010; 22: 238-244.
[24] Condamine T and Gabrilovich DI. Molecular mechanisms regulating myeloid-derived suppressor cell differentiation and function. Trends Immunol 2011; 32: 19-25.
[25] Saiwai H, Kumamaru H, Ohkawa Y, Kubota K, Kobayakawa K, Yamada H, Yokomizo T, Iwa-

moto Y and Okada S. Ly6C+ Ly6G- Myeloid-derived suppressor cells play a critical role in the resolution of acute inflammation and the subsequent tissue repair process after spinal cord injury. J Neurochem 2013; 125: 74-88.
[26] Ribechini E, Greifenberg V, Sandwick S and Lutz MB. Subsets, expansion and activation of myeloid-derived suppressor cells. Med Microbiol Immunol 2010; 199: 273-281.
[27] Davies D. Cell separations by flow cytometry. Methods Mol Med 2001; 58: 3-15.
[28] Ma C, Kapanadze T, Gamrekelashvili J, Manns MP, Korangy F and Greten TF. Anti-Gr-1 antibody depletion fails to eliminate hepatic myeloid-derived suppressor cells in tumor-bearing mice. J Leukoc Biol 2012; 92: 1199-1206.
[29] Liu ZX, Han D, Gunawan B and Kaplowitz N. Neutrophil depletion protects against murine acetaminophen hepatotoxicity. Hepatology 2006; 43: 1220-1230.
[30] Xia S, Sha H, Yang L, Ji Y, Ostrand-Rosenberg S and Qi L. Gr-1+ CD11b+ myeloid-derived suppressor cells suppress inflammation and promote insulin sensitivity in obesity. J Biol Chem 2011; 286: 23591-23599.
[31] Ribes S, Regen T, Meister T, Tauber SC, Schutze S, Mildner A, Mack M, Hanisch UK and Nau R. Resistance of the brain to Escherichia coli K1 infection depends on MyD88 signaling and the contribution of neutrophils and monocytes. Infect Immun 2013; 81: 1810-1819.
[32] Youn JI, Kumar V, Collazo M, Nefedova Y, Condamine T, Cheng P, Villagra A, Antonia S, McCaffrey JC, Fishman M, Sarnaik A, Horna P, Sotomayor E and Gabrilovich DI. Epigenetic silencing of retinoblastoma gene regulates pathologic differentiation of myeloid cells in cancer. Nat Immunol 2013; 14: 211-220.